

Dental laser research: selective ablation of caries, calculus, and microbial plaque From the idea to the first in vivo investigation

Peter Rechmann, Prof. Dr. med. dent.

*Department of Preventive and Restorative Dental Sciences, Division of Clinical General
Dentistry, University of California San Francisco, 707 Parnassus Avenue,
San Francisco, CA 94143, USA*

Dental practitioners can use color to differentiate between healthy and diseased tooth structures. Absorption of laser light is one of the most important factors in laser tissue interaction, and different dental tissues display varying absorption characteristics. Two questions can be posed: (1) Would it make sense to study the absorption differences between carious and healthy tooth structures? (2) Can a laser be used for the selective removal of caries based on natural differences in absorption? These ideas have led to numerous research projects and several patented inventions.

Absorption characteristics of enamel, dentin, and carious dentin in the visible and ultraviolet spectral domain

At the beginning of this research, little data existed regarding absorption characteristics of dental hard tissues. In 1983, Nagasawa's light transmission data from dental hard substances showed that selective ablation of caries based on "natural" absorption differences would not be possible with lasers emitting in the infrared spectrum. Using a light source emitting wavelengths between 1 μm and 12.5 μm (1000–12,500 nm), he demonstrated that absorption in healthy dentin is higher than absorption in carious dentin [1].

This work was partially supported by the North Rhine Westphalia ministry of Science and Technology.

E-mail address: rechmannp@dentistry.ucsf.edu

Because that finding is the opposite of the author's goal, a measurement of the absorption of carious and healthy enamel and dentin by the ultraviolet and visible light spectrum was undertaken. The optical density of healthy and carious dentin and enamel was measured by using microspectrophotometry (Fig. 1). The curves represent the optical densities of carious lesions, healthy dentin, and enamel and show that in the wavelength range of 240 to 770 nm, carious lesions demonstrate a stronger absorption than healthy dentin and enamel.

Combining those absorption curves for healthy and carious dentin into a single line shows the relative absorption between caries and dentin for each wavelength measured (Fig. 2). In the spectral range of 320 to 520 nm, the optical density and absorption of carious dentin is four times higher than for healthy dentin [2–5]. The conclusion is that a laser wavelength within this spectral domain would allow ablation of carious dentin. Thus, the window of promising wavelengths for selective ablation of carious tooth structures was found.

Optoacoustic determination of ablation thresholds

The next step was to prove that, using light energy in the wavelength range of 320 to 520 nm, selective ablation of diseased dentin is possible while ensuring that healthy tissue remains untouched. That task was tackled by determination of the ablation thresholds of carious and healthy dentin. An optoacoustic measuring approach was used to determine the ablation thresholds of healthy and carious dentin [3,5,6]. The ablation threshold defines the onset of removal of material when increasing energy is applied to the substance. Subthreshold energies produce only heating up of the substance, which results in a minimal volumetric expansion. This change can be measured as a pressure wave with a sensitive microphone. At the ablation

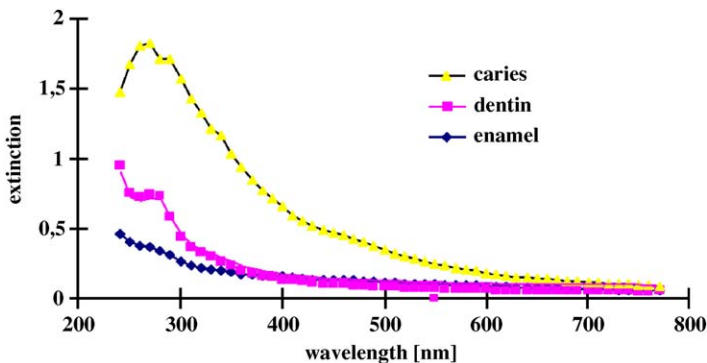


Fig. 1. Absorption spectra of enamel and carious and healthy dentin in the ultraviolet and visible spectral domain.

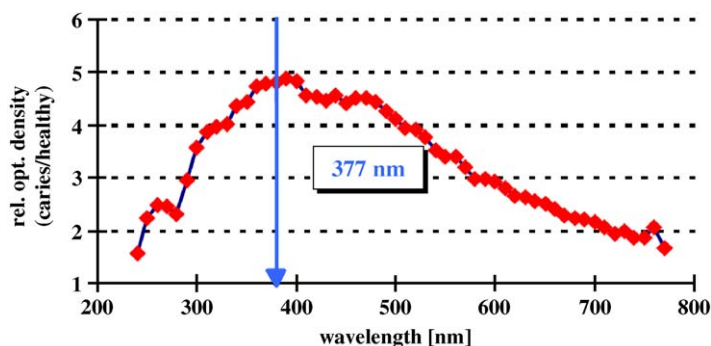


Fig. 2. Relative absorption ratio of carious and healthy dentin.

threshold, the explosive removal of material causes a sudden rise in the detected pressure. The measured pressure curve changes from a gradual rise into a much steeper slope.

The ablation thresholds for carious and healthy dentin were determined using lasers emitting in the blue spectral range where the absorption differences between carious and healthy dentin were the highest. The two devices were (1) a frequency-tripled Nd:YAG laser emitting a wavelength of 355 nm, with a pulse duration 9 nanoseconds, q-switched, and (2) a frequency-doubled Alexandrite laser emitting at 377 nm with a pulse duration 200 nanoseconds, q-switched [3–5,7,8]. Fig. 3 shows the results for the frequency-doubled Alexandrite (fdA) laser. The left curve illustrates the measured pressure curve for carious dentin. At low energies pressure is detected at low levels, and at about 0.4 J/cm² the steepness of the curve suddenly rises, defining the ablation threshold of carious dentin. The right

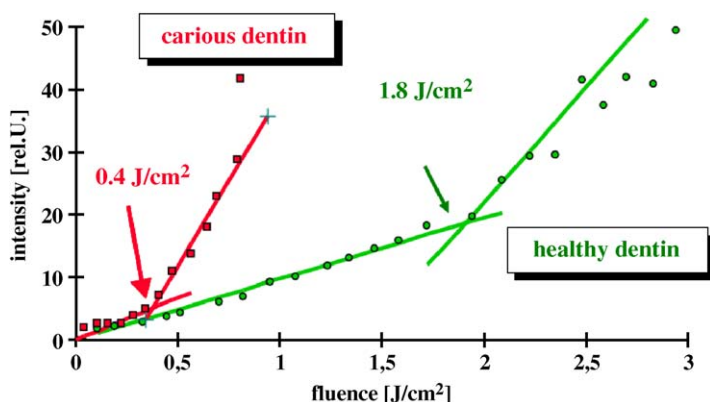


Fig. 3. Optoacoustic determination of ablation threshold of carious dentin (left curve) and healthy dentin (right curve); fdA laser.

curve demonstrates the threshold for healthy dentin at 1.8 J/cm^2 . This result demonstrates that selective ablation of caries is possible when the applied energies are at least 0.4 J/cm^2 but below 1.8 J/cm^2 . Using that energy window, caries should be removed and sound dentin is unaffected.

Verification of selectivity

After finding the window of wavelengths and the appropriate energy range for selective ablation of caries, the next steps are to determine whether ablation is selective and to study the rate of ablation above different thresholds.

To measure ablation activity, a sensitive nontactile microtopography method was developed, similar to that of a CD player “reading” differences in height in a CD track. Using that measuring tool, the determination of the ablation rates in carious and healthy dentin for any given fluence was possible [9]. The fdA laser was used in contact with a fiber delivery system.

Initial fluence of 0.6 J/cm^2 was applied to carious and healthy dentin. Although the ablation rate in carious dentin was measured at $0.18 \mu\text{m}$ per laser pulse, 100 laser pulses onto healthy dentin resulted in no ablation. This demonstrates that applying fluence just above the determined ablation threshold for caries allows selective ablation (Fig. 4).

Fig. 5 displays the same situation for fluence just below the ablation threshold of healthy dentin. At 1.5 J/cm^2 healthy dentin is not ablated, but the ablation rate in carious dentin is increased to $2.2 \mu\text{m}$ per laser pulse.

Fig. 6 shows the result of fluence applied just above the ablation threshold of healthy dentin. Using 2 J/cm^2 , $2.7 \mu\text{m}$ of carious and $0.02 \mu\text{m}$ of healthy dentin are removed per laser pulse.

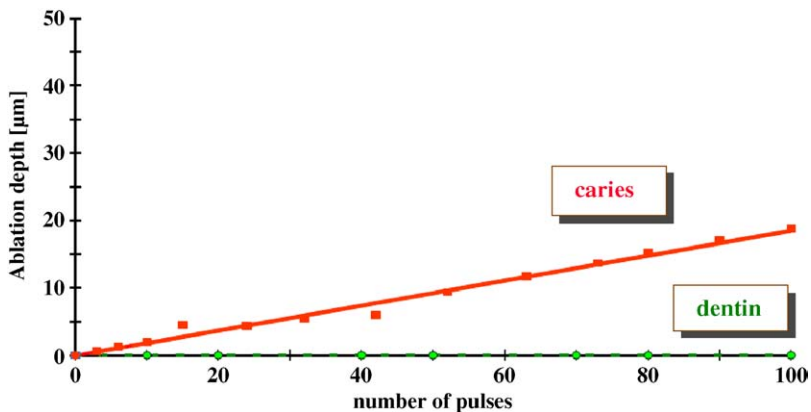


Fig. 4. Ablation efficiency of carious and healthy dentin; fdA laser (0.6 J/cm^2).

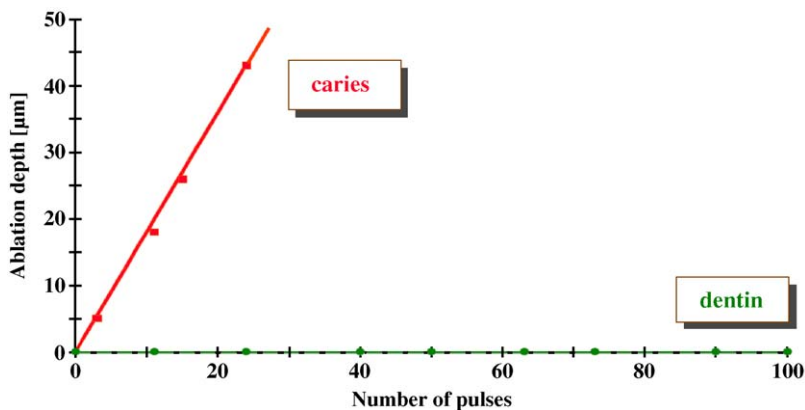


Fig. 5. Ablation efficiency of carious and healthy dentin; fdA laser (1.5 J/cm²).

Fig. 7 shows the optoacoustic determination of ablation thresholds mentioned above but extends the scale on both axes, displaying the same measured curve. Data points at higher fluences reveal that there is an additional second sudden change in the slope marking a second ablation threshold for healthy and carious dentin. These second ablation thresholds are found at fluences twice those of the first ablation thresholds [6,8–10]. Previously, there were only a few studies mentioning this phenomenon [11–13], and the assumption was made that up to the second ablation threshold a “desorption” process takes place [9]; that is, low energy causes a loss of thin layers from the surface. Using energies beyond the second ablation threshold, bulk removal via thermal explosion occurs.

The determination of ablation efficiency revealed that the results of the optoacoustic-determined ablation thresholds and the microtopographic

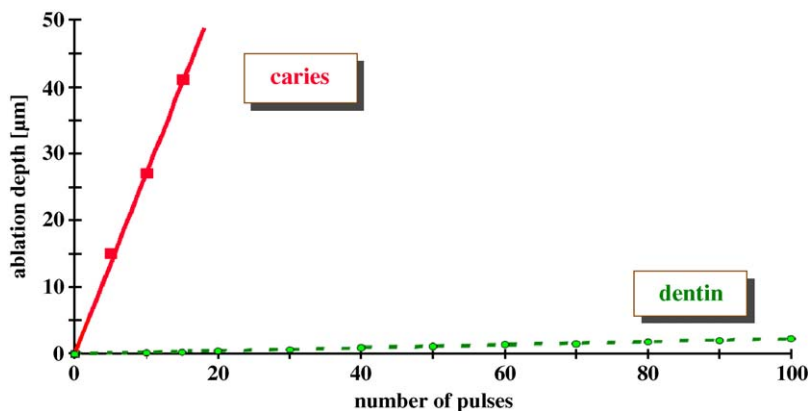


Fig. 6. Ablation efficiency of carious and healthy dentin; fdA laser (2.0 J/cm²).

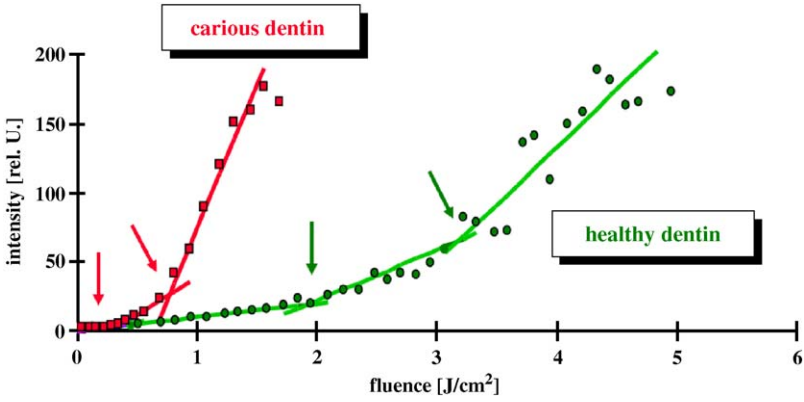


Fig. 7. Optoacoustic determination of ablation threshold of carious dentin (*left curve*) and healthy dentin (*right curve*); fdA laser, extended scale on both scales. Two ablation thresholds are marked.

measurements correspond. The microtopographic measurements verified different ablation speeds below and above those thresholds. Fig. 8 shows the ablation efficiency for carious and healthy dentin at a fluence just below the second ablation threshold for healthy dentin. At 3.2 J/cm² the ablation efficiency in carious dentin rises to 9.25 μm per pulse and is more than 100 times the ablation efficiency of healthy dentin (0.06 μm/pulse). If the applied fluence is raised above the second ablation threshold for healthy dentin, the efficiency in healthy dentin increases (Fig. 9).

Table 1 summarizes the ablation rates below and above the different ablation thresholds for carious and healthy dentin. Using a laser with a repetition rate of 100 to 150 Hz allows for fast and effective removal of caries in the second energy window. This second energy parameter,

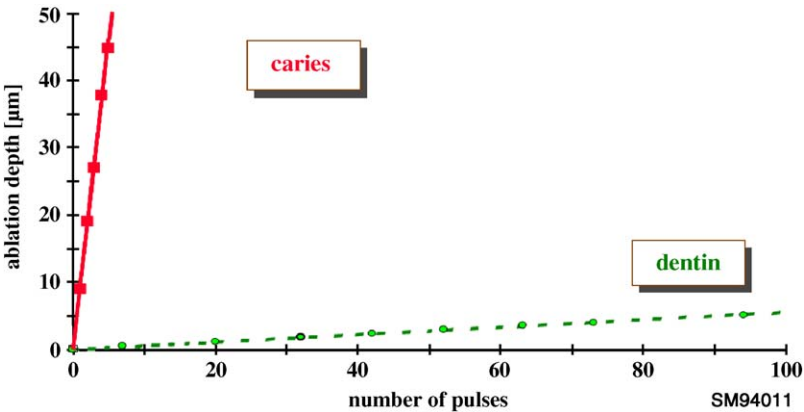


Fig. 8. Ablation efficiency of carious and healthy dentin; fdA laser (3.2 J/cm²).

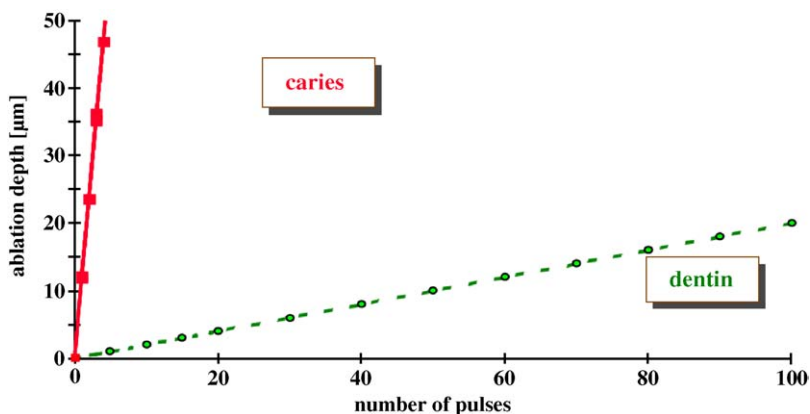


Fig. 9. Ablation efficiency of carious and healthy dentin; fdA laser (4.0 J/cm²).

representing a “99% selectivity” mode, can be used to remove the bulk of caries. When approaching the pulp, the system could be switched down to the “total selective” regime by applying energies below the first ablation threshold of healthy dentin to ensure that it is not removed.

Temperature in the pulp chamber

All laser ablation processes are thermal interactions, and heat accumulates in the tissue. The next research step was to evaluate the relationship between the different irradiation parameters and temperature rise in the pulp chamber. The question was which maximum pulse repetition rate might be applied to produce rapid ablation with a minimal temperature rise in the pulp chamber.

Measurements were performed in a small sample chamber where the “room” temperature was set to 30.5°C and where relative humidity was kept at 90%. Fig. 10 shows the experimental setup using the fdA laser (100 nanosecond pulse duration, q switched) equipped with a 300-µm contact

Table 1
Ablation efficiency at fluences below and above the first and second ablation thresholds for carious and healthy dentin

Fluence (J/cm ²)	Carious dentin ablation rate (µm/pulse)	Healthy dentin ablation rate (µm/pulse)
0.6	0.18	0.00
1.5	2.20	0.00
2.0	2.71	0.02
3.2	9.25	0.06
4.0	11.7	0.20

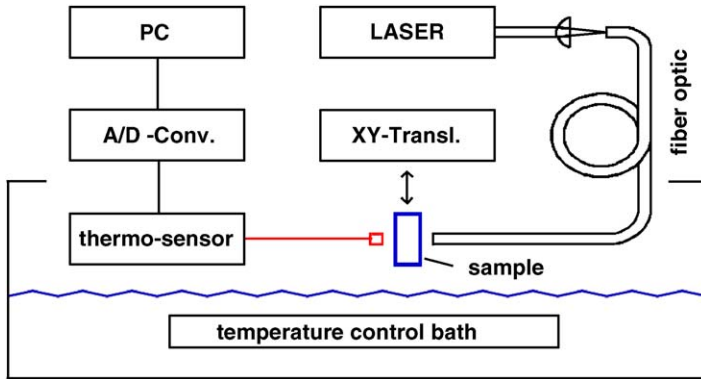


Fig. 10. Experimental set-up for temperature measurements.

fiber. No water cooling was used. The temperature was measured with a thermocouple located behind the dentin slice on the side opposite to the laser irradiation. This way a defined remaining dentin thickness was simulated [14].

Thermographic measurements: typical temperature profiles over time

Fig. 11 shows a typical temperature curve measured over time. The lower curve demonstrates the temperature rise at the back of a 0.9-mm-thick dentin slice, and the upper curve demonstrates the situation behind a simulated 0.2-mm remaining dentin thickness. During the delivery of laser energy, the temperature increases dramatically in the first 6 seconds; after 15 seconds, the steepness of the temperature curve starts to flatten. A plateau is reached at 3.5 minutes.

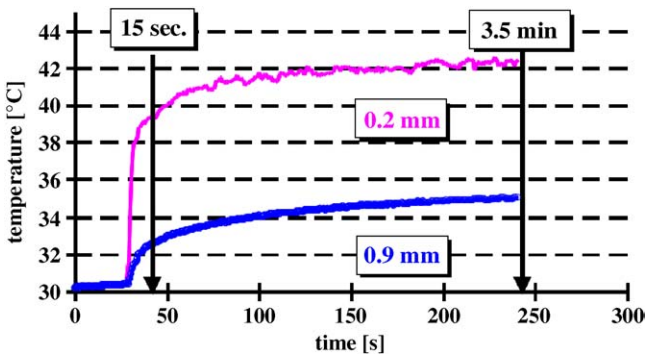


Fig. 11. Temperature measurement over time (dentin thickness 0.2 and 0.9 mm).

Thermographic measurements at variable fluences

To evaluate the effect of applied fluence to temperature rise, a 0.9-mm remaining dentin thickness was chosen. The pulse repetition rate was set to 20 Hz. The temperature was recorded after 6 seconds of irradiation. This small interval of irradiation was chosen because it causes only 60 μm loss of dentin at highest applied energy. (Too much loss of material falsifies the temperature measurement because the distance to the sensor is reduced.)

A linear relationship between applied fluence and temperature increase in the pulp chamber is observed (Fig. 12). The temperature rise at the first ablation threshold is about 2.3°C and at the second is 4.8°C. The linear increase is independent of the ablation thresholds, and the steepness of the line is about 1.3°C/J/cm². These results were not expected because application of subthreshold energies usually leads to a higher heat accumulation compared with energies above an ablation threshold. This experiment shows that the absorbed photon energy is transferred nearly completely into heat [14]. This idea is supported by similar observations from Neev et al [15] and Hibst et al [16].

Determination of temperature increase as a function of dentin thickness

Fig. 13 shows the relation between thickness of dentin and temperature increase. The two lines represent the two different measuring times (after 15 seconds and after 3.5 minutes). The temperature increase was 17°C at a distance of 0.1 mm, 7°C at 0.5 mm, and 3°C at 2 mm, all after 3.5 minutes of irradiation without cooling [14,17].

From the viewpoint of clinical relevance, the distance of 0.5 mm to the pulp can be taken as limit for safety calculations and further measurements.

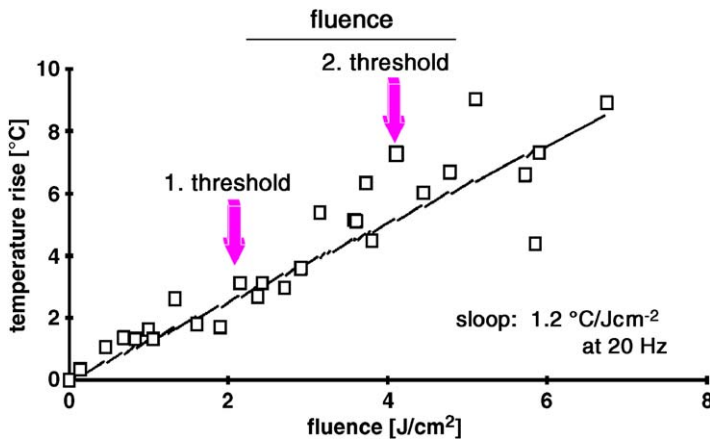


Fig. 12. Temperature increase after 6 seconds of irradiation at various fluences.

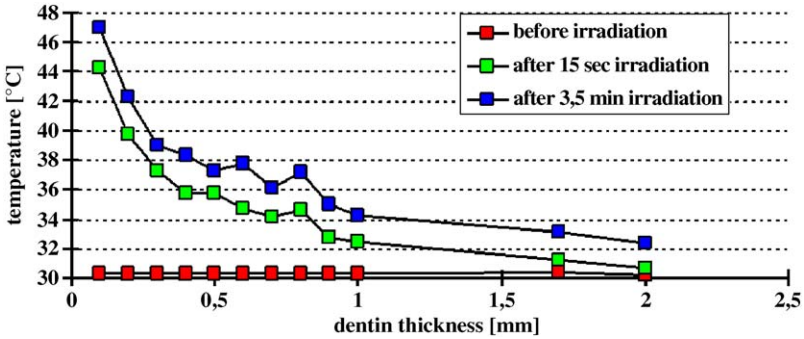


Fig. 13. Temperature increase as a function of dentin thickness.

If the carious lesion extends to within 0.5 mm of the pulp, the pulpal tissue is deemed to be irreversibly irritated [18], and any further irritations by temperature rise seem to be clinically irrelevant. Murray et al [19] stated that the remaining dentin thickness should be at least 0.5 mm to avoid evidence of pulp injury.

Determination of temperature increase as a function of pulse repetition rate

The irradiations with different pulse repetition rates were applied to the same location to keep the measurements free of uncertainties arising from any variations in the probe area. To reduce an accumulation of heat in the dentin slices with repetition rates up to 120 Hz, water cooling was applied (30 mL/minute, 24.5°C). In Fig. 14, the temperature increase after 3.5 minutes of irradiation at 2 J/cm² is plotted versus pulse repetition rate. The

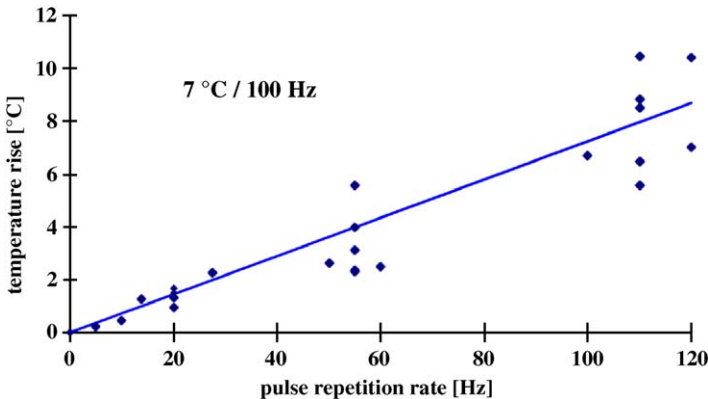


Fig. 14. Temperature increase as a function of pulse repetition rate (dentin thickness 0.8 mm, fluence 2 J/cm²).

curve shows that the temperature increase per 1 Hz is 0.11°C at a “remaining” dentin thickness of 0.8 mm. The temperature increase at 20 Hz is about 2.2°C and at 120 Hz is about 13.2°C [14].

Fig. 15 illustrates the relationship between temperature rise and pulse repetition rate over a 20-minute period. The dentin thickness is 0.8 mm, and 2 J/cm^2 is used with water cooling. With the water temperature of 24.5°C , the dentin slice temperature increases 3°C almost immediately after the laser energy is applied. After several minutes, the repetition rate was decreased to 10 Hz, and the measured temperature dropped 1.5°C . The laser repetition rate was re-established several times at 20 Hz, and each time the same 3°C temperature increase was achieved. When the repetition rate decreased to a fourth or an eighth of the original, the temperature rise dropped by the same factor. Immediately after turning off the laser, the temperature at the back of the dentin slice returned to the original water temperature [17]. For clinical use, an important question is how low a water temperature would be acceptable for the patients.

Histologic investigations of dental hard tissues after a 377-nm laser impact

Thus far the experiments determined the basic laser parameters for a selective ablation of caries based on natural differences in absorption and demonstrated the relationship between different fluences, pulse repetition rates, remaining dentin thickness, water cooling, and the temperature rise of the pulp chamber. The next step in the line of investigations deals with the histologic appearance of a cavity after selective caries removal with the fDA laser.

Fig. 16 shows a light microscopic view of two holes prepared into carious dentin on decalcified sections. The borders of the craters are well defined. Figs. 17 and 18 show the applied laser energy increased to 2 J/cm^2 , which resulted in ablation of healthy dentin. In Fig. 17, laser energy was applied to

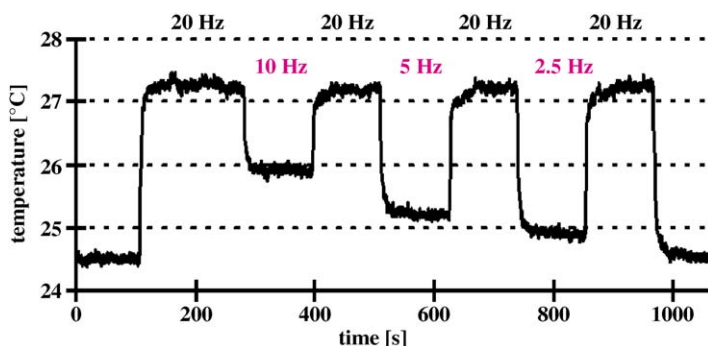


Fig. 15. Relationship of temperature rise to pulse repetition rate (water cooling 30 mL/minute; water temperature 24.5°C ; pulse repetition rate 2.5, 5, 10, and 20 Hz; fluence 2 J/cm^2).

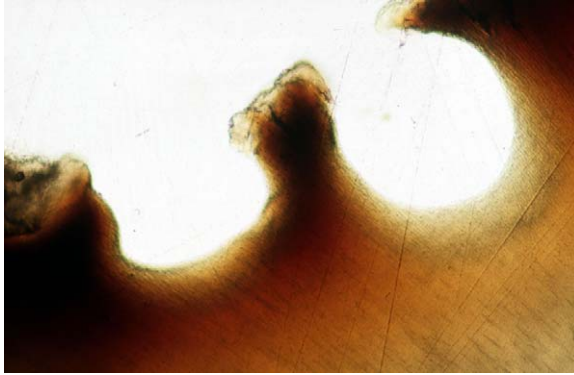


Fig. 16. Carious dentin after laser preparation of two holes exhibiting well-defined borders (light microscopic view, undecalcified sections).

the dentinal tubules parallel to their long axes, and there is a smooth border of the ablation crater with a micro roughness of about 10 μm . In Fig. 18, the laser energy is applied perpendicular to the tubules' axes. In this case, the zone of micro roughness is extended up to 25 μm in width. The laser applications were done under water with 100-nanosecond pulses, using two repetition rates: 20 Hz and 110 Hz (55 Hz, double spikes, spike to spike distance 30 μs) [20–22].

After laser irradiation of dentin, some sections were stained with toluidine blue (Fig. 19). The stainable zone has a width of less than 60 μm , which represents a change in collagen due to the thermal effect. There is a zone next to the laser impact where the dentinal tubules seem to be empty. At the greater repetition rate, neither carbonization zones due to excessive heat nor micro cracks could be observed.

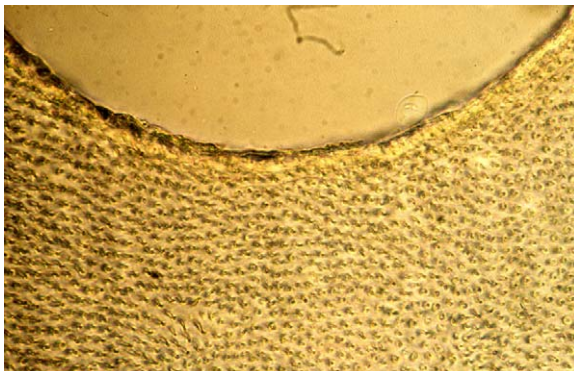


Fig. 17. Crater prepared in healthy dentin, laser energy directed at dentinal tubules parallel to their axes, 10- μm roughness (light microscopic view, undecalcified sections).

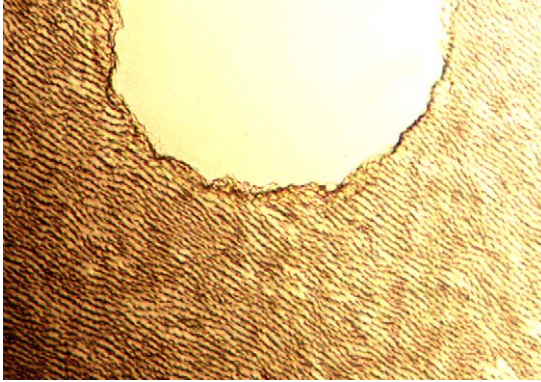


Fig. 18. Crater prepared in healthy dentin, laser energy directed at dentinal tubules perpendicular to their axes, 25- μm roughness (light microscopic view, undecalcified sections).

A scanning electron microscopic (SEM) picture of a crater prepared in soft carious dentin is presented in Fig. 20. The margins are sharp and well defined; in longitudinal direction there are some opened dentinal tubules. After caries is totally removed, the remaining dentin shows no smear layer; and the dentinal tubules are wide open (Fig. 21).

Selective ablation of caries: the handpiece

Caries selective therapy is restricted to fluences defined by the ablation thresholds of carious and healthy dentin. The laser energy must be delivered uniformly to the lesion surface. Noncontact delivery systems produce an uneven beam profile with differing energies at the point of the irradiation. Alternatively, contact fiber delivery systems offer homogenous laser energy

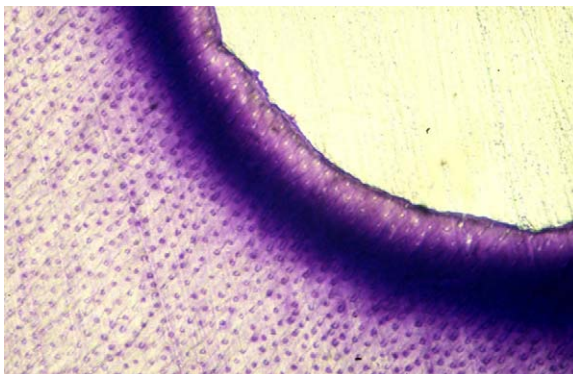


Fig. 19. Toluidine blue-stained zone around an ablation crater in dentin, 60 μm in width.

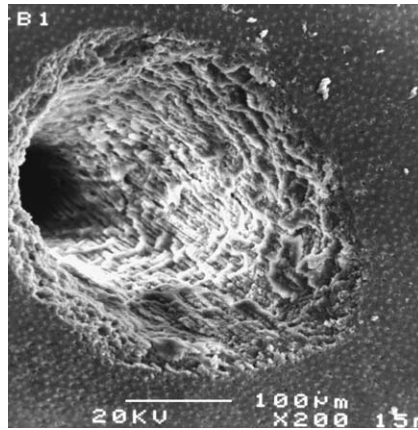


Fig. 20. SEM view of a crater lasered into carious dentin.

within the fiber diameter. The drawback of a typical fiber system is that, when used in contact, its surface can be altered after a few laser pulses due to particles repelling back from the ablation area. That could change the energy distribution.

To prevent the immediate destruction of its surface, the distal end of the fiber was placed inside a small metallic tube [23]. Water flows around the side of the fiber and exits the metal tube as a laminar stream and prevents repelled particles from striking the fiber surface. After more than 2 hours and 12,000 laser pulses of testing, there was no change in the fiber surface after use, and the beam profile was still homogeneous [24].

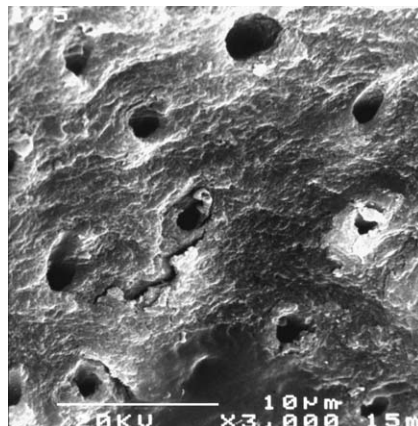


Fig. 21. SEM view of dentin after laser preparation. Dentinal tubules are wide open, no smear layer is visible.

In addition to providing protection, the water delivers effective cooling directly to the target tissue point. This allows fast and effective ablation with pulse repetition rates of 100 Hz and up; moreover, as long as the water stream remains laminar, the laser light is guided inside the water stream.

A shift in thinking

During the experiments, it became obvious that the visible color of caries was not the important factor for the preferred absorption of laser light in the spectral region between 320 and 520 nm because “white” caries was also ablated selectively [3–5]. Moreover, dark-stained secondary dentin was not ablated when selective laser energy was applied.

These were the first hints that the important absorption factor for selective ablation of caries is not the color seen by the naked eye. The search for a method of laser calculus removal and minimally invasive periodontal therapy revealed that selective ablation of carious tooth structure and selective ablation of calculus is based on the absorption of the blue laser energy by bacteria.

Fluorescence emission measurements for selective removal of calculus

Fluorescence emission measurements on samples exhibiting calculus and dentin were performed [25–27]. Fig. 22 shows that calculus starts emitting light of about 420 nm when it is irradiated with an excitation wavelength of 337 nm (N_2 laser). For simplification, all wavelengths between the excitation wavelength and the above-mentioned fluorescence wavelength are those that are absorbed by the target substance. Therefore, the conclusion is that calculus absorbs light up to a wavelength of 420 nm, whereas healthy dentin absorbs up to 370 nm.

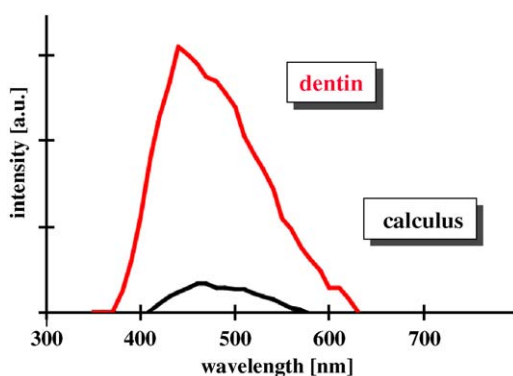


Fig. 22. Fluorescence emission spectra of healthy dentin and subgingival calculus; excitation wavelength 337 nm (N_2 laser).

These fluorescence measurements revealed that calculus favorably absorbs wavelengths up to 420 nm and that dentin is much less absorbing in that wavelength spectrum [28]. A window of wavelengths for selective ablation of calculus was found, demonstrating benefits to using the fdA laser.

Selective removal of microbial plaque and calculus: histologic evaluations

To prove that selective ablation of calculus is possible using a wavelength between 337 and 420 nm, histologic investigations were performed on teeth extracted due to severe periodontitis and on freshly surgically removed impacted third molars. All teeth were mounted on a motor-driven x-y-z table. During irradiation, the table was moved in the z-direction, resulting in an irradiated stripe on the tooth surface. To identify the irradiated portion of the sample during histologic examination, a hole was drilled perpendicular to and beyond that area (Fig. 23). Portions of enamel, the cemento-enamel junction, and cementum and dentin on the root were irradiated.

The fdA laser parameters were 100-nanosecond pulse duration, repetition rate of 110 Hz (55 Hz, double spikes, spike-to-spike distance 30 μ s), 1 J/cm² fluence, irradiation time between 0.1 and 2 seconds, water cooling, and spot size of 500 μ m.

The lateral aspect of an extracted lower incisor with two irradiated stripes is shown in Fig. 24. The irradiated stripes appear clean, and the healthy surface is untouched.

Fig. 25 shows a thin layer of calculus, and Fig. 26 demonstrates a large mass of supragingival calculus located on the enamel. The laser removed the calculus, and the underlying enamel was untouched in both cases.

Fig. 27 demonstrates the situation at the cementum enamel junction, where scaling with hand instruments or ultrasonic devices can be challenging. In different samples it was shown that laser removal of calculus was successful, with no harm to the underlying structures.

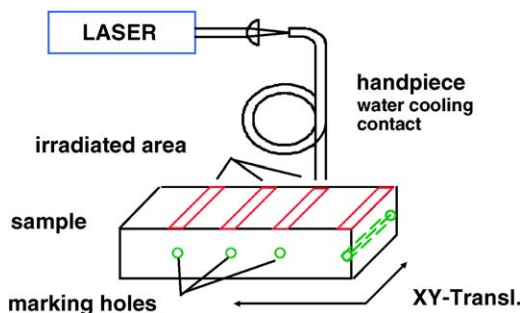


Fig. 23. Experimental set-up for irradiation of a tooth surface; x-y-motor driven translation table; marking holes drilled perpendicular beyond irradiation stripes.



Fig. 24. Lateral aspect of an extracted lower incisor with two irradiated cleaned stripes.



Fig. 25. Thin layer of supragingival calculus on enamel. Calculus is removed where laser is used (light microscopic view).

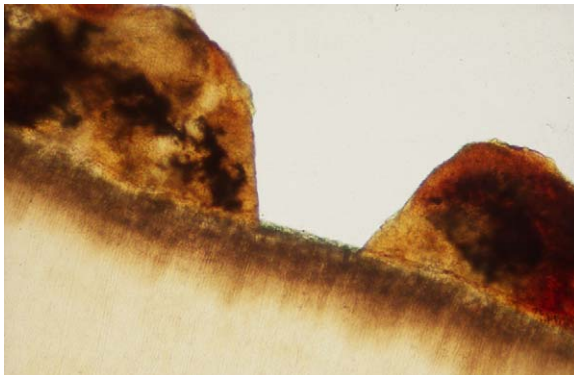


Fig. 26. Thickened supragingival calculus on enamel. Calculus is removed where laser is used (light microscopic view).

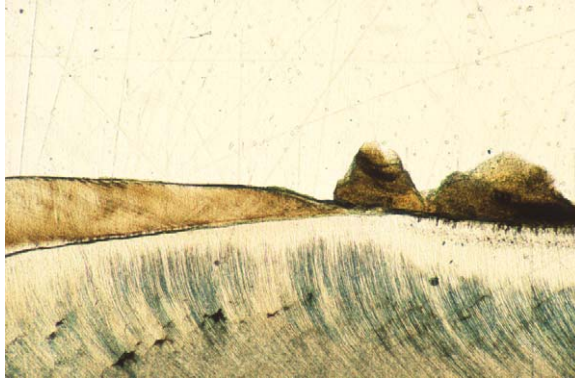


Fig. 27. Laser impact at the cementum enamel junction. Calculus is removed; no harm to the underlying structure occurred (light microscopic view).

Figs. 28 and 29 demonstrate with higher magnification the situation after irradiation of calculus located on cementum. The cementum and underlying dentin remains untouched while the calculus is removed. In other portions of the study, irradiation with selective ablation parameters was performed over longer periods of time (up to hours). In each case, after the removal of calculus, there were no observable changes in the underlying tissues.

Light microscopic evaluations revealed that selective calculus removal is possible using a blue laser like the fdA instrument [25–27,29–32]. The experiments revealed that dark-colored subgingival and light-colored supragingival deposits are easily removed. Moreover, experiments showed that bacteria-laden microbial plaque could easily be removed with a fdA

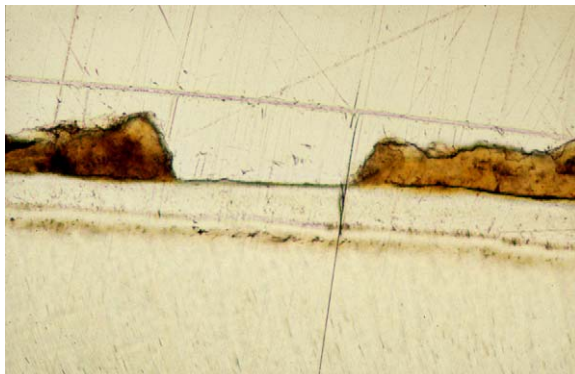


Fig. 28. Laser removal of subgingival calculus from cementum. Calculus is removed; no alteration of cementum is visible (light microscopic view).

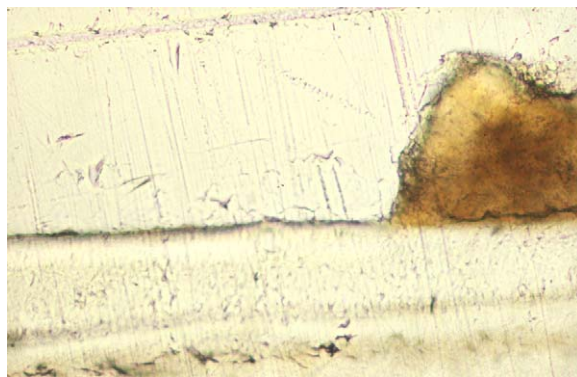


Fig. 29. Higher magnification of image in Fig. 28. No alterations in cementum are detectable.

laser (Fig. 30), providing an additional hint that bacteria might be the main absorbing agent.

Selective removal of calculus: electron microscopic investigations

Scanning electron microscopic analysis was used on similar samples using laser parameters identical to the histologic investigations [33–35]. Fig. 31 demonstrates two parallel irradiation stripes on the lateral aspect of the clinical crown of an upper incisor, showing a completely cleaned enamel surface. At the higher magnification in Fig. 32, total calculus removal is demonstrated. The border to the noncleaned surface and pits in the enamel from the beginning of earlier carious acid attacks are visible.

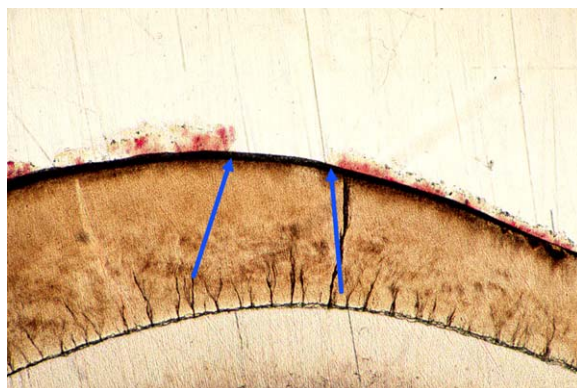


Fig. 30. Laser removal of microbial plaque on enamel. Arrows mark the irradiation area (light microscopic view).

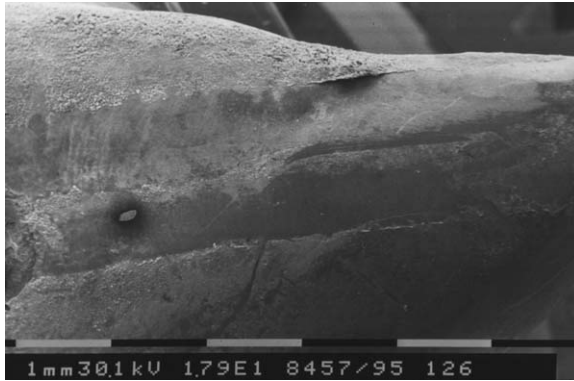


Fig. 31. Two irradiation stripes on enamel. Enamel surface is cleaned (SEM view).

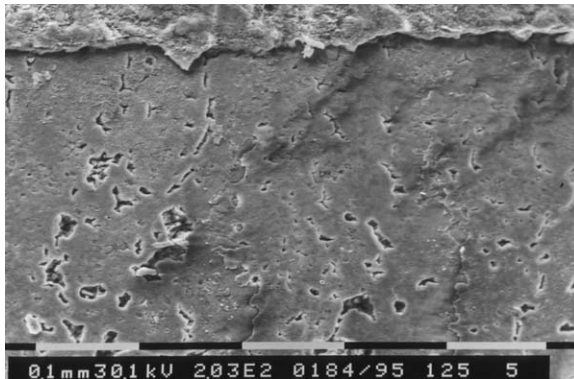


Fig. 32. Higher magnification of enamel surface. Enamel is cleaned (SEM view).



Fig. 33. Overview of an irradiated stripe in the region of enamel, the enamel cementum junction, and the root surface (from left to right) (SEM view).

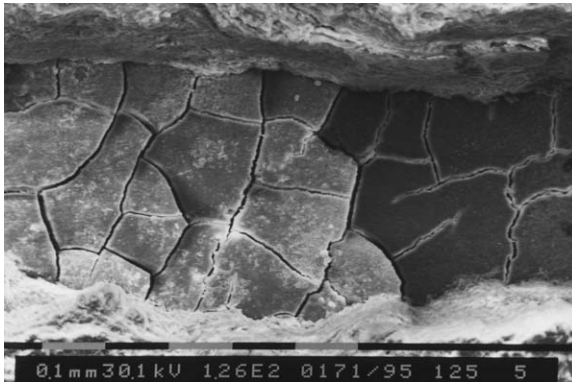


Fig. 34. Higher magnification of image in Fig. 33. Calculus is cut off sharply. At the bottom of the canyon-like stripe, cementum is cleaned (SEM view).

Fig. 33 shows an overview of an irradiated stripe in thick calculus, and Fig. 34 demonstrates the cementum part of that track at high magnification. The irradiated surface includes the enamel, the cementum enamel junction (exhibiting massive first-acid attacks), and the cementum (left to right). The stripe shows calculus removed cleanly and sharply, and in the region of the bulky calculus, the track appears “canyon-like.” The cementum surface at the bottom of the track is cleaned and exhibits a smooth surface (cracks in cementum can be observed in treated and untreated areas all over the tooth and are due to the preparation procedure for the SEM).

Fig. 35 demonstrates the situation after irradiation of the cementum surface of an unerupted third molar in high magnification. Layers of fibrous tissue are visible. The cementum was irradiated in a typical manner as described above. In all healthy cementum samples, no differences between

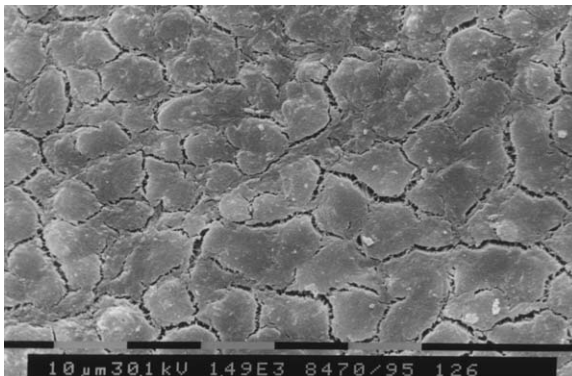


Fig. 35. Cementum surface of an unerupted third molar, partially irradiated. No difference is visible between irradiated and unirradiated area (SEM view).

treated and nontreated cementum surfaces were obvious, and the healthy cementum remains untouched.

Selective ablation of calculus: the approach into the periodontal pocket

Fig. 36 shows a schematic drawing of the outlet of the application handpiece. The fiber resides inside the metal tube, and water flows between the fiber and the metal tube. Optical fibers have different numerical apertures (NA) defining the escape angle of the light at the fiber tip. In this case the NA is 0.1. Assuming that fluences for selective ablation are between 1.5 and 3.0 J/cm², this handpiece design offers that range of fluence from the tip up to a distance of 2 cm.

In Fig. 37, the tip of a 600- μ m handpiece is projected into a schematic periodontal pocket. The calculus in a periodontal pocket can be reached because of the “conical” irradiation geometry. It seems reasonable to state that calculus detected with a periodontal probe is easily reached with the fiber. Smaller application tips will be designed to reach deep in between furcation areas.

Bacterial reduction

Selective ablation of dark and white caries, supra- and subgingival calculus, and microbial plaque is possible using a “blue” laser. Another scientific step in the research path is to prove whether bacteria would be

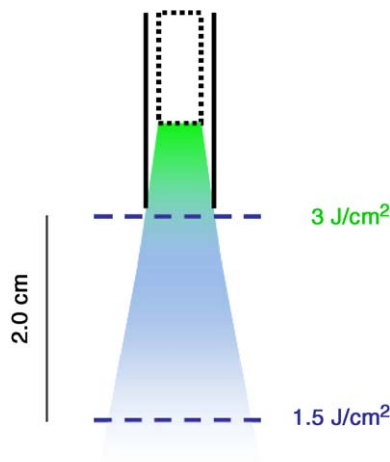


Fig. 36. Schematic drawing of the outlet of the application handpiece. The “irradiation cone” with appropriate energy is illustrated, and limits (1.5–3 J/cm²) for selective ablation of calculus are marked.

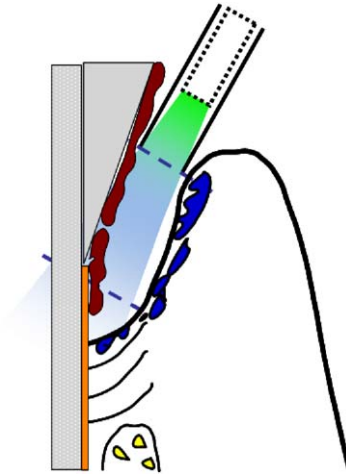


Fig. 37. Tip of the handpiece projected into a schematic sulcus.

influenced by the irradiation and, for purposes of the author's research, whether the fdA laser can achieve that goal.

Laboratory strains of *Escherichia coli* and *Bacteroides vulgaris* were irradiated while placing them into an optical transparent buffer solution (no absorption of 377 nm wavelength) (Fig. 38). A fluence of 0.02 J/cm^2 was projected through a microtiter plate containing the suspended bacteria. Fig. 39 shows the dose-dependent killing of bacteria. Only a fraction of 1% of bacteria survive at a dose of $1.4 \times 10^6 \text{ J/m}^2$, which is the value typically applied during a periodontal treatment (one pocket area, treatment time 90 seconds, average power 1.5 W). After applying a dose of $5 \times 10^6 \text{ J/m}^2$, no viable germs were found [36,37].

Because bacteria in such optically transparent solutions are difficult to manipulate, more research needs to be done in the area of bacterial reduction with blue laser light.

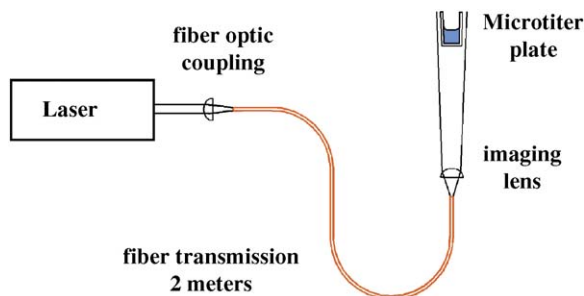


Fig. 38. Experimental set-up for irradiation of bacteria suspended in a microtiter plate.

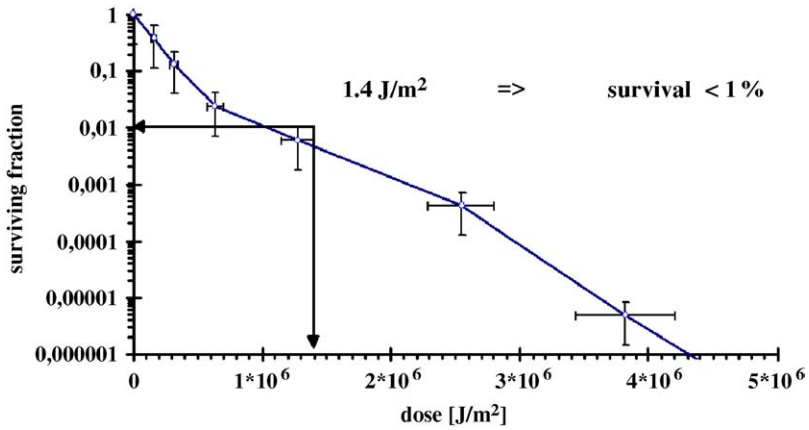


Fig. 39. Surviving fractions of *E coli* after irradiation of bacteria suspension (wavelength 377 nm, fluence 0.02 J/cm²). Dose-dependent bacterial reduction is observed.

Measurement of the efficiency of calculus removal in a human mouth model

A simulated gingival sulcus model was designed and built. This study compared treatment efficiency for subgingival calculus removal between the fdA laser (1 microsecond pulse duration, pulse repetition rate 70 Hz, and water cooling) and an ultrasonic cleaning device (Sonosoft Lux tip #9; KaVo, Biberach, Germany). Extracted teeth with subgingival calculus were placed on a model plate. Standardized pictures were taken, and silicone rubber was placed to simulate the gingival pocket conditions (Fig. 40). After treatment, the rubber was removed, and pictures were taken and compared with the beginning photographs to ascertain the amount of calculus removed.

The results showed that the laser treatment time for subgingival calculus removal was approximately 30% longer than ultrasonic scaling followed by

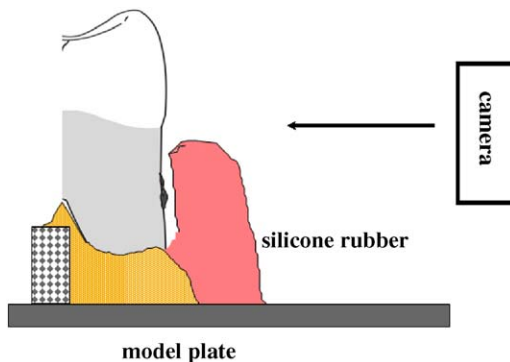


Fig. 40. Human mouth model simulating gingival pocket conditions.

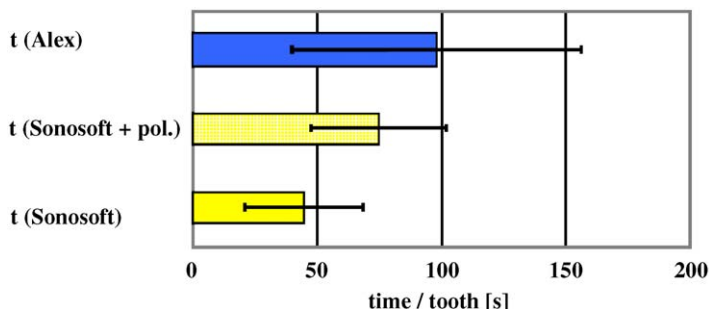


Fig. 41. Average removal time of calculus on human teeth in the mouth simulation model; treatment time for ultrasonic device without and with polishing and fdA laser.

polishing (Fig. 41). However, the amount of residual calculus left behind after ultrasonic cleaning was 11% to 14%. In contrast, an average of 1% to 2% of residual calculus remained after the laser treatment. The prolonged treatment time is less important than the efficient removal of calculus (Fig. 42) [38,39].

Periodontal treatment in dogs: a pulpal safety study

The pulpal safety study was performed on four adult Labrador dogs. This study's intention was to prove that the selective ablation of calculus with the fdA laser would be safe for the dental pulp. The parameters used were pulse duration 1 microsecond, pulse repetition rate 70 Hz, and water cooling. In each dog, nine teeth in the lower and upper jaw were irradiated with three different fluences for 4 minutes per tooth. The chosen fluences were up to four times higher than necessary for selective ablation of calculus (1.5, 3, and 6 J/cm²). Using the worst-case scenario for pulpal overheating, irradiation was performed perpendicular to the root surface at the enamel

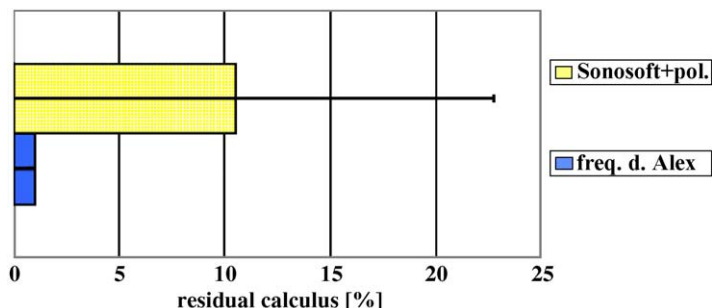


Fig. 42. Average amount of residual calculus using an ultrasonic device including polishing versus fdA laser.

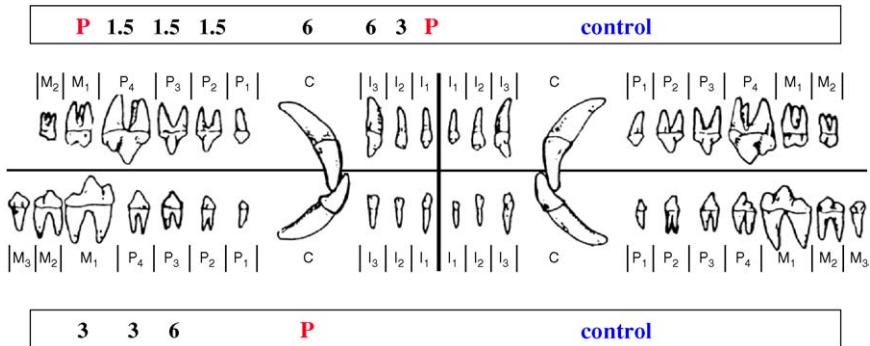


Fig. 43. Periodontal treatment in dogs; irradiation scheme for pulpal safety study; irradiation with fluences of 1.5, 3, and 6 J/cm²; positive and control teeth.

cementum junction; the buccal surface was irradiated after the gingiva was reflected with a modified Widman flap. At three other sites, deep fillings were placed as positive controls. All teeth from the opposite quadrants served as negative controls. Fig. 43 shows the irradiation scheme.

During the observation period, no dogs showed clinical gingival inflammation or abscess formation. Moreover, the animals demonstrated no signs of pain, discomfort, or abnormal behavior.

Dogs were killed after 1 day or 1, 4, or 6 weeks. The histologic evaluations of all treated teeth showed no acute or chronic reactions; no alterations in the odontoblast layer; no hyperemia or infiltration; and no signs of mild, moderate, or severe inflammation. This was true for all irradiation parameters, even when fluences four times higher than those necessary for the selective ablation of calculus were applied [40,41].

Summary

The results show that using a laser that emits laser light in the blue spectral region and applying appropriate fluences allows for selective ablation of disease. The frequency-doubled Alexandrite laser is one such instrument.

References

- [1] Nagasawa A. Research and development of lasers in dental and oral surgery. In: Astumi K, editor. *New frontiers in laser medicine and surgery*. Amsterdam, Oxford: Exerpta Medica; 1983. p. 233–41.
- [2] Rechmann P, Hennig T. Untersuchungen zur selektiven Kariesabtragung mit gepulsten Lasern. *ZWR* 1993;102:637–42.
- [3] Hennig T, Rechmann P, Pilgrim C, Schwarzmaier H-J, Kaufmann R. Caries selective ablation by pulsed lasers. *SPIE Proc Lasers Orthop Dental Vet Med* 1991;1424:99–105.

- [4] Hennig T, Rechmann P, Pilgrim C, Kaufmann R. Basic principles of caries selective ablation by pulsed lasers. In: Powell GL, editor. Proceedings of the ISLD third international congress on lasers in dentistry. Salt Lake City, (UT): University of Utah Printing Service; 1992. p. 119–20.
- [5] Rechmann P, Hennig T, Kaufmann R. Laser in der zahnhartsubstanzabtragung: grundlagen, möglichkeiten und aussichten. *ZWR* 1992;101:150–60.
- [6] Rechmann P, Hennig T, Jeitner P. Ablationskennlinien von dentin: 377 nm versus 755 nm. *Dtsch Zahnarztl Z* 1994;49:142–4.
- [7] Rechmann P, Hennig T, von den Hoff U, Kaufmann R. Caries selective ablation using a 2nd harmonic alexandrite-laser. In: Powell L, editor. Proceedings of the Third International Congress on Lasers in Dentistry. Salt Lake City (UT): ISLD; 1992. p. 123–4.
- [8] Rechmann P, Hennig T, von den Hoff U, Kaufmann R. Caries selective ablation: wavelength 377 nm versus 2.9 μm . *SPIE Proc Laser Orthop Dental Vet Med* 1993;1880:235–9.
- [9] Hennig T, Rechmann P, Jeitner P, Kaufmann R. Caries selective ablation: the second threshold. *SPIE Proc Laser Orthop Dental Vet Med* 1993;1880:117–24.
- [10] Rechmann P, Hennig T. Ablation characteristics of healthy dentin at different laser wavelengths. *SPIE Proc Laser Orthop Dental Vet Med* 1994;1984:38–43.
- [11] Muller G, Scholz C, Ertl T. Basic laser tissue interaction with special emphasis on bone and dental treatment. *Innov Tech Biol Med* 1990;2:4–5.
- [12] Feuerstein O, Palanker D, Fuxbrunner A. Effect of the ArF-excimer laser on human enamel. In: Powell GL, editor. Proceedings of the ISLD third international congress on lasers in dentistry. Salt Lake City (UT): University of Utah Printing Service; 1992. p. 261–2.
- [13] Feuerstein O, Palanker D, Fuxbrunner A, Lewis A, Deutsch D. Effect of the ArF excimer laser on human enamel. *Lasers Surg Med* 1992;12:471–7.
- [14] Hennig T, Rechmann P, Holtermann A. Caries selective ablation: temperature in the pulp chamber. *SPIE Proc Laser Surg* 1994;2128:397–402.
- [15] Neev J, Liaw LH, Raney DV, Fujishige JT, Ho PD, Berns MW. Selectivity, efficiency, and surface characteristics of hard dental tissues ablated with ArF pulsed excimer lasers. *Lasers Surg Med* 1991;11:499–510.
- [16] Hibst R. Mechanical effects of erbium:YAG laser bone ablation. *Lasers Surg Med* 1992;12: 125–30.
- [17] Hennig T, Rechmann P, Holtermann A. Selektive kariesabtragung: messungen zur temperaturerhöhung im pulpakavum. *Dtsch Zahnarztl Z* 1994;49:154–6.
- [18] Beetke E, Wenzel B. Zur Caries profunda und deren therapeutische consequenzen. hanser verlag. *Deutscher Zahnartzkalender* 1992;51:41–56.
- [19] Murray PE, Smith AJ, Windsor LJ, Mjor IA. Remaining dentine thickness and human pulp responses. *Int Endod J* 2003;36:33–43.
- [20] Hennig T, Rechmann P, Jeitner P. Effects of a 2nd harmonic Alexandrite-laser on human dentin. *SPIE Proc Int Conference Adv Laser Dent* 1994;1984:24–30.
- [21] Rechmann P, Hennig T. Caries selective ablation: first histological examinations. *SPIE Proc Laser Surg* 1994;2128:389–96.
- [22] Rechmann P, Hennig T. Histological investigation of dental hard tissues after 377 nm laser impact. *Lasers Dent* 1995;4:101–5.
- [23] Hennig T, Rechmann P, Holtermann A. Caries selective ablation: the handpiece. *SPIE Proc Lasers Dent* 1995;2394:196–202.
- [24] Hennig T, Rechmann P. Improved performance of selective ablation using a specially designed handpiece. *SPIE Proc Med Applications Lasers* 1996;2623:180–8.
- [25] Rechmann P, Hennig T, Spengler B. Selective ablation of subgingival calculus. In: Loh Hong-Sai, editor. Proceedings of the 4th International Congress on Lasers in Dentistry. Singapore: Monduzzi Editore; 1995. p. 159–62.
- [26] Rechmann P, Hennig T. Selective ablation of sub- and supragingival calculus with a frequency-doubled Alexandrite laser. *SPIE Proc Lasers Dent* 1995;2394:203–10.

- [27] Rechmann P, Hennig T. Selective ablation of dental calculus with a frequency-doubled Alexandrite laser. *SPIE Proc Med Applications Lasers* 1995;2623:180–8.
- [28] Fink F, Kaschke I. Laserspektroskopische verfahren der kariesdiagnostik. In: Zuhrt R editor. *Laseranwendung in der zahn-, mund- und kieferheilkunde*. Landsberg FRG: Ecomed; 1994.
- [29] Rechmann P, Hennig T. A frequency doubled Alexandrite-laser for selective ablation of dental calculus: first investigations. In: Loh Hong-Sai, editor. *Proceedings of the 4th International Congress on Lasers in Dentistry*. Singapore: Monduzzi Editore; 1995. p. 95–100.
- [30] Rechmann P, Hennig T, Goldin DS. Calculus removal with an Er:YAG laser and a frequency doubled alexandrite laser. In: Powell GL, editor. *Proceedings of the 6th International Congress on Lasers in Dentistry*. Salt Lake City (UT): University of Utah; 1999. p. 218–22.
- [31] Rechmann P, Hennig T. Lasers in periodontology, today and tomorrow. *Med Las Applic* 2001;16:223–30.
- [32] Rechmann P, Hennig T. Lasers in periodontology new trends. *J Oral Laser Applic* 2002; 2:1–8.
- [33] Rechmann P, Hennig T, Sadegh HMM, Goldin DS. Light and scanning electron microscope investigations comparing calculus removal using an Er:YAG laser and a frequency doubled Alexandrite laser. *SPIE Proc Laser Dent* 1997;2973:53–9.
- [34] Rechmann P, Hennig T. SEM investigations of the cementum surface after irradiation with a frequency-doubled Alexandrite laser. *SPIE Proc Lasers Dent* 1996;2672:176–80.
- [35] Rechmann P, Hennig T. Frequency doubled Alexandrite laser for use in periodontology: a scanning electron microscopic investigation. *SPIE Proc Med Applications Lasers* 1996; 2922:107–12.
- [36] Hennig T, Rechmann P, Pecnik T, Heinz H-P, Hadding U. Influence of second harmonic alexandrite-laser radiation on bacterial growth. *SPIE Proc Lasers Dentistry* 1996;2672:40–5.
- [37] Rechmann P, Hennig T. Influence of 2nd harmonic Alexandrite-Laser radiation on bacteria. In: Powell GL, editor. *Proceedings of the 6th International Congress on Lasers in Dentistry*. Salt Lake City (UT): University of Utah; 1999. p. 225–7.
- [38] Pilgrim C, Rechmann P, Goldin DS, Hennig T. Measurement of efficiency in calculus removal with a frequency doubled Alexandrite laser on pig jaws. *SPIE Proc Lasers Dent* 2000;3910:50–8.
- [39] Pilgrim C, Rechmann P, Goldin DS, Hennig T. Comparison of calculus removal with an ultrasonic device and a frequency-doubled Alexandrite laser on pig's teeth and on extracted human teeth. In: Nammour S, editor. *7th International Congress on Lasers in Dentistry abstract handbook*. Brussels (Belgium): ISLD; 2000. p. 39.
- [40] Rechmann P, Hennig T, Reichart P. Periodontal treatment with the frequency doubled alexandrite laser in dogs. *SPIE Proc Lasers Dent* 2000;3910:35–41.
- [41] Rechmann P, Hennig T, Reichart P. Dental pulp reaction after irradiation with a frequency doubled Alexandrite laser in dogs. In: *7th International Congress on Lasers in Dentistry abstract handbook*. Brussels (Belgium). 2000. p. 41.